Review article

# Comparison of $^{60}$Co and $^{192}$Ir sources in HDR brachytherapy

Stefan Strohmaier, MSc[1], Grzegorz Zwierzchowski, MSc, PhD[2]

[1]University of Applied Sciences, Technikum Wien Medical Engineering, Vienna, Austria, [2]Department of Medical Physics, Greater Poland Cancer Centre, Poznan, Poland

## Abstract

This paper compares the isotopes $^{60}$Co and $^{192}$Ir as radiation sources for high-dose-rate (HDR) afterloading brachytherapy. The smaller size of $^{192}$Ir sources made it the preferred radionuclide for temporary brachytherapy treatments. Recently also $^{60}$Co sources have been made available with identical geometrical dimensions. This paper compares the characteristics of both nuclides in different fields of brachytherapy based on scientific literature. In an additional part of this paper reports from medical physicists of several radiation therapy institutes are discussed. The purpose of this work is to investigate the advantages or disadvantages of both radionuclides for HDR brachytherapy due to their physical differences. The motivation is to provide useful information to support decision-making procedures in the selection of equipment for brachytherapy treatment rooms. The results of this work show that no advantages or disadvantages exist for $^{60}$Co sources compared to $^{192}$Ir sources with regard to clinical aspects. Nevertheless, there are potential logistical advantages of $^{60}$Co sources due to its longer half-life (5.3 years vs. 74 days), making it an interesting alternative especially in developing countries.

J Contemp Brachyther 2011; 3, 4: 199-208
DOI: 10.5114/jcb.2011.26471

**Key words:** $^{60}$Co, $^{192}$Ir, HDR brachytherapy, radionuclides.

## Purpose

The use of high-dose-rate (HDR) afterloading brachytherapy is a highly widespread practice today. It has proven to be a successful treatment for cancers of the prostate, cervix, endometrium, breast, skin, bronchus, oesophagus, head and neck and several other types of cancer. Up to now the production of small sources for HDR afterloading was only possible for iridium-192, because of technological reasons. The smaller size of the sources allowed interstitial treatment and optimization of dose. This made $^{192}$Ir the most used isotope for HDR afterloading brachytherapy worldwide. Recently $^{60}$Co sources became available with identical geometrical dimensions as miniaturized $^{192}$Ir sources. These two radionuclides show different physical characteristics, while $^{60}$Co offers logistical and economic advantages. Typical intervals for source replacements foresee 25 source exchanges for $^{192}$Ir compared to just a single one for $^{60}$Co, resulting in reduced operating costs as a result of a longer half-life, 5.3 years ($^{60}$Co) compared to 74 days ($^{192}$Ir). Especially in developing countries frequent source exchanges may be challenging in view of the available infrastructure.

## Radionuclides in brachytherapy

Many radionuclides have a history as a source for brachytherapy, but today only a few are commonly used. They are characterized by the rate at which their strength decays (half-life), by how much radioactivity can be obtained for a given mass of the radioactive source (specific activity) and by the energies and types of the radiation particles that are emitted from the source (energy spectrum) [1].

### *Half-life*

The strength of a radiation source decays exponentially. The half-life is the time it takes for the source strength to decay to half of its initial value. The half-life of a specific source determines how long it can be used over a period of time. Sources with short half-lives can reduce the risks of radiation exposure around the patient, because the radiation decreases rapidly in time. When it comes to dose calculation the decay of the source may not be explicitly accounted for if the source has a long half-life. For example, $^{137}$Cs sources, with a half-life of 30 years, are assumed to keep constant source strength during the treatment period of a few days, whereas the dose calculation for $^{125}$I sources, with a half-life of just 59.49 days, needs to consider the decay of the sources during the time of the implant. The activity of an isotope is defined as its decay per unit of time.

### *Specific activity*

The specific activity is the ratio of activity contained within a unit mass of the source. The strength of a brachy-

**Address for correspondence:** Stefan Strohmaier, MSc, c/o: Dipl. Ing. Peter Tonhäuser, Eckert+Ziegler Bebig GmbH, Berlin, phone: +49 30 941084 297, fax: +49 30 941084 630, ✉ e-mail: peter.tonhaeuser@bebig.eu

Received: 14.06.11
Accepted: 12.12.11
Published: 31.12.11

therapy source for practical applications is limited by its specific activity. When a parent nuclide is activated in a neutron flux field, the number of radioactive nuclides per unit mass that may be obtained is limited by the neutron flux field strength, the parent's nuclide neutron cross-section, and the source's half-life. This is important for HDR interstitial brachytherapy applications, which require small source dimensions as well as high source strengths. $^{192}$Ir sources are very popular because of its high specific activity and high neutron cross-section [2].

### *Energy*

The average energy of a brachytherapy source determines the penetrability of the photon particles emitted from the source. High energy sources allow a higher dose to tissues at larger distances to the sources, but require thicker shielding for protection of the staff. Low-energy photon emitting sources, such as $^{125}$I and $^{103}$Pd, are often used for permanent brachytherapy treatments, because the radiation of these sources is mostly diminished by the patient's tissue. When high-energy sources, such as $^{198}$Au, are used, the patient needs to stay in the hospital until the source strength decays to a suitable value, such that the radiation exposure outside the patient satisfies state regulations [3]. The thickness of any materials that reduce the exposure by 50% is known as the half-value layer (HVL) [4]. In general, intracavitary irradiation requires more penetration in tissue than interstitial brachytherapy. Sources adequate for intracavitary applications should have radial dose functions which do not fall rapidly with distance. $^{137}$Cs, $^{192}$Ir and $^{60}$Co would be suitable candidates, because all of them emit relatively high-energy photons [5].

## Dosimetry in brachytherapy

Accurate determinations of dosimetric characteristics of brachytherapy sources are very important. The dosimetric characteristics can be determined by using appropriate experimental techniques and dosimeters. Theoretical calculations are also very useful in the determination of dosimetric characteristics of brachytherapy sources [6, 7].

### *Experimental techniques*

Dose measurement in brachytherapy requires accurately positioned detectors, which produce measurable signals that have known relationship to the relative or absolute dose in the medium in the absence of the detector. Detectors commonly used in brachytherapy are thermoluminescent detectors (TLDs), radiochromic films, plastic scintillators and thermoluminescent (TL) sheets. The dose distribution of brachytherapy sources is characterized by large dose gradients and a large range of dose rates. A suitable detector must have a wide dynamic range, flat energy response, small size and high sensitivity. Another challenge is the variation of detector response with a change in source to detector distance [6-10].

## AAPM TG43 algorithm

The dose distribution in the vicinity of a brachytherapy source is a complex function of the emitting energy spectra, the geometry of the source and the material close to the source. The most established dosimetry protocol for dose calculation in brachytherapy has been elaborated by the American Association of Physicists in Medicine (AAPM) for the dosimetry in the vicinity of radiation sources. Most reviews on newly introduced radionuclides are based on this dosimetry method. The TG-43 approach consists of using measured and Monte Carlo generated dose-rate distributions directly for clinical dose calculation aided by a standard table-lookup formalism. Today most treatment planning software vendors have implemented the TG-43 formalism and the recommended parameters in their systems [11-13]. The radial dose fall-off from any gamma source, the rate at which dose decreases with increasing distance from the source, is determined by:

### *Geometry factors*

For a point source of radiation, the dose decreases approximately as the square of the distance from the source. Radioactive sources used in brachytherapy are not point sources; they are typically linear sources. For these linear sources the decrease in dose falls more as the first power of the distance, rather than the square of the distance.

### *Attenuation*

The dose rate also decreases with increasing distance from the source, because of attenuation of the gamma rays by the intervening tissues or environment [14].

### *General 2D formalism*

The dose rate $D(r,\theta)$ of a cylindrically symmetric source X (X = L for a line source and X = P for a point source) at an arbitrary point $F(r,\theta)$ follows the following equation:

$$\dot{D}(r,\theta) = S_k \times \Lambda \times \frac{G_x(r,\theta)}{G_x(r_o,\theta_o)} \times g_x(r) \times F(r,\theta)$$

$r$ – distance (in centimetres) from the centre of the active source to the point of interest,

$r_0$ – denotes the reference distance which is specified to be 1 cm,

$\theta$ – polar angle specifying the point of interest, P $r$, $\theta$ , relative to the source longitudinal axis, $\theta_0$ – reference plane defines the source transverse plane, and is specified to 90°,

$S_k$ – source strength specified in air kerma strength,

$\Lambda$ – dose rate constant defined as the ratio of the dose rate at the reference point; the dose rate constant can be evaluated by using a calculation method such as the Monte Carlo method,

$G_x(r,\theta)$ – geometry factor that describes the effect of the active source material distribution within the source on the dose distribution outside the source,

$g_x(r)$ – radial dose function accounting for the effects of absorption and scatter on the dose distribution in the medium along the transverse axis of the source,

$F(r,\theta)$ – anisotropy factor describes the effects of anisotropic photon attenuation, by the source material or

materials away from the source transverse axis. Geometric factors may cause the dose to be direction-dependent [15] (Fig. 1).

### *Experimental dosimetry versus Monte Carlo*

The main disadvantage of experimental dosimetry is the positioning of the detectors near the sources (distances less than 1 cm from the source). The high dose gradient that appears near the source and the poor signal-noise ratio for great distances away from the source affect the accuracy. On the other hand, Monte Carlo calculation accuracy can be affected by inaccuracies in the geometric configuration of the source, uncertainties in the cross-sections and the modelling of the physical processes in the Monte Carlo code. Monte Carlo calculations can be verified by measuring a set of points where experimental uncertainties are relatively low. An important aspect is how to validate the comparison of Monte Carlo with measurements. For non-low energy radionuclides such as $^{60}$Co and $^{192}$Ir, it is accepted that results can be validated by comparison with experimental results for a source of the same radionuclide and similar design. But for low energy sources it is recommended to do the validation for the same source model, because the dependence on source geometry and materials is very significant. Further verification of the geometric data of the source provided by the manufacturer is recommended. This can be done by contact radiography, special cameras or microscopy [6-8, 15].

### *$^{60}$Co and $^{192}$Ir sources in HDR afterloading gynaecological brachytherapy*

Richter *et al*. compared a $^{60}$Co and a $^{192}$Ir source of identical dimension and construction and discussed tissue absorption, geometry function and integral dose of the two sources. The cobalt source consists of a metallic $^{60}$Co cylinder with a length of 3.5 mm and a diameter of 0.6 mm. The source is surrounded by a cylindrical steel jacket and an outer diameter of 1 mm [16]. The results of the calculation of the differences between the two sources are shown in Fig. 2. For instance, the dose for $^{60}$Co sources in fat tissue is 0.4 percent higher and 0.8 percent lower for the rectum than for $^{192}$Ir sources. The largest difference is found in lung tissue, with 2.1%. The biological response difference to the different energies of the $^{60}$Co and $^{192}$Ir sources are therefore negligible [16].

Figure 3 shows the anisotropy factor $\Phi(\theta)$ as in practice parameterization of the $r$ dependence is introduced for simplification and the anisotropy factor $F(r,\theta)$ is reduced to $\Phi(\theta)$ at the distance $r$ = 4 cm. The $^{60}$Co source shows advantages as the $^{192}$Ir source shows deviations at the top of the source ($\theta$ = 0°) and at the source mounting ($\theta$ = 180°) [16].

The radial dose function depends on the phantom size. Figure 4 shows the results for both line sources in an infinite phantom. Like in an ideal point source, the initial fall of the radial dose function of the iridium source is less steep than the cobalt source. This relation reverses at distances greater than 22 cm as a result of the higher photon energy of $^{60}$Co. This also explains that although the integral dose in the patient is slightly lower, higher room shielding is required for the use of $^{60}$Co sources in brachytherapy. The influence of the phantom size on the radial dose is shown in Fig. 5; near the surface of the spherical phantom with the radius of 15 cm a reduction of the radial dose is clear [16].

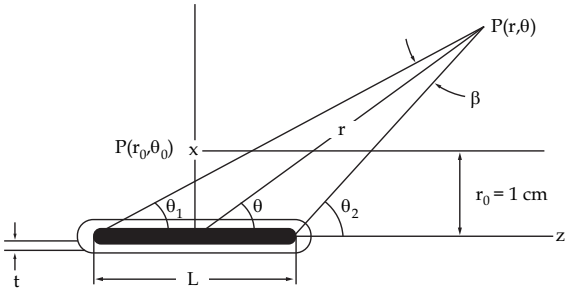


**Fig. 1.** Encapsulated line source, illustrating calculation of the dose rate at point P(r,θ) = P(x,y) relative to the source centre. The source length and encapsulation thickness are denoted by $L$ and $t$ [15]

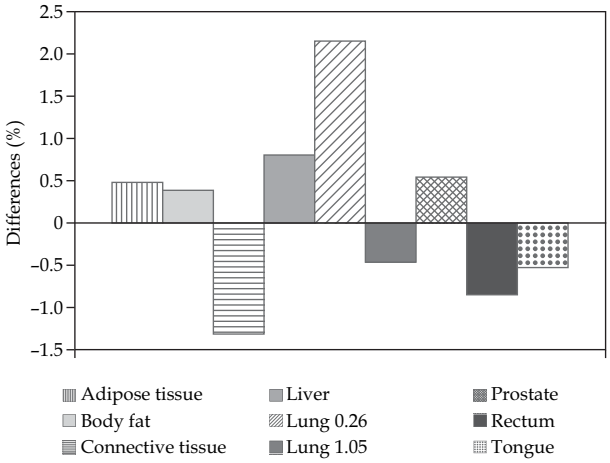


**Fig. 2.** Differences in absorbed dose of several tissues for a $^{60}$Co source in comparison to a $^{192}$Ir source [16]

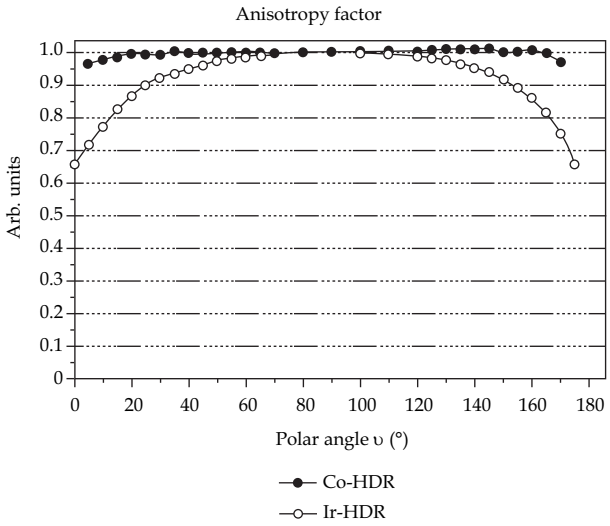


**Fig. 3.** Anisotropy factor $\Phi(\theta)$ for the $^{60}$Co and $^{192}$Ir source [16]

Richter *et al.* also show an almost identical dose distribution for the reviewed $^{60}$Co and $^{192}$Ir sources. In Fig. 6 an equal dose distribution for a combination of a ring-shaped and linear applicator is demonstrated [16].

Park *et al.* [17] also compared the dose distributions of three radiation sources and two treatment planning systems in HDR intracavitary brachytherapy. In Figs. 7 and 8 the radial dose function and the anisotropy function used for the study of the HDR sources are shown. Figure 7 shows that the influence of different phantom size and the physical difference between $^{60}$Co and $^{192}$Ir are distinguished from those of the geometrical difference on the radial dose function. Figure 8 shows that the effect of a physical difference is also bigger than that of a geometrical difference. High penetration of gamma rays emitted from $^{60}$Co represents a wide difference in the source tip and the region connected to the source cable in this figure.

### *Dose at large distances from $^{60}$Co and $^{192}$Ir brachytherapy sources*

Ionization chamber measurements were performed in a water tank to describe the decrease of dose with distance of the mentioned sources. As an independent check of the results, Monte Carlo calculations with the EGS-4 code system were executed in a simulated water phantom. The dimensions of the water tank were changed to simulate different patient sizes. The decrease of the dose around a brachytherapy source is mainly described by the inverse square law. Within the first few centimetres this is accurate. But at 10 cm deviations from the inverse square law may be as large as 20%, depending on the energy of the emitted radiation. The relationship between the tissue attenuation factor $T(r)$ and the radial dose function $g(r)$ is discussed in a report of the AAPM Radiation Therapy Committee Task Group No. 43 [18]. For point source geometry and energies > 300 keV, there is a very close relationship between the two functions, so that $g(r)$ equals $T(r)$ normalized at the distance of $r_0$ = 1 cm.

Venselaar *et al.* [19] investigated three isotopes: $^{60}$Co, $^{192}$Ir and $^{137}$Cs. Only the results for $^{60}$Co and $^{192}$Ir are considered, because $^{137}$Cs is not of relevance in HDR brachytherapy anymore. Both $^{60}$Co and $^{192}$Ir have a long history in intracavitary brachytherapy. The sources used in the study consisted of two $^{60}$Co sources with a total activity of 89 GBq and a $^{192}$Ir source with a nominal activity of

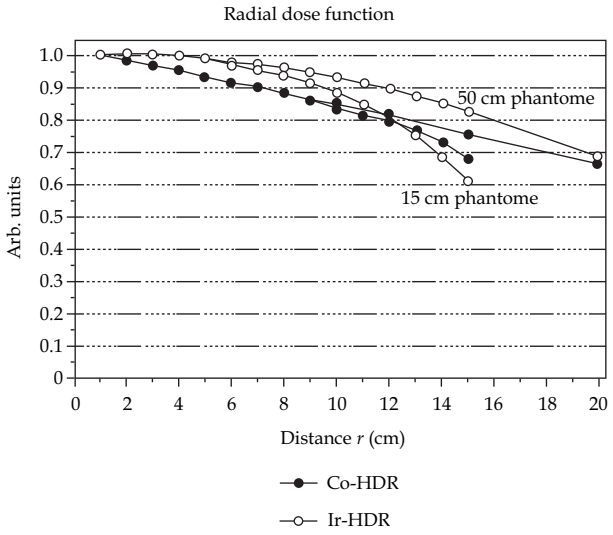


**Fig. 4.** Radial dose function of $^{60}$Co and $^{192}$Ir source [16]

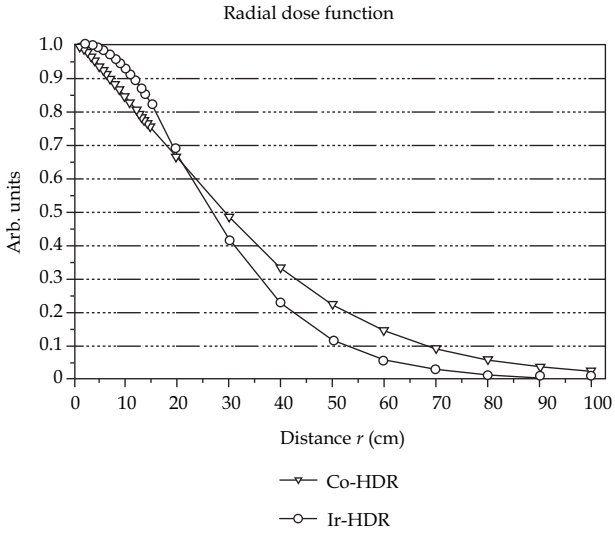


**Fig. 5.** Radial dose functions for greater distances from the source in an infinite phantom [16]

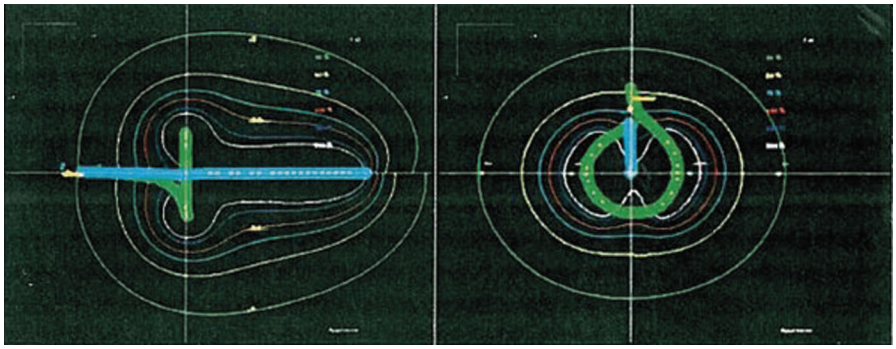

**Fig. 6.** Dose distribution for $^{60}$Co and $^{192}$Ir source of a ring-shaped and linear applicator for the irradiation of a cervical carcinoma (upper half depicting $^{192}$Ir, lower half $^{60}$Co) [16]

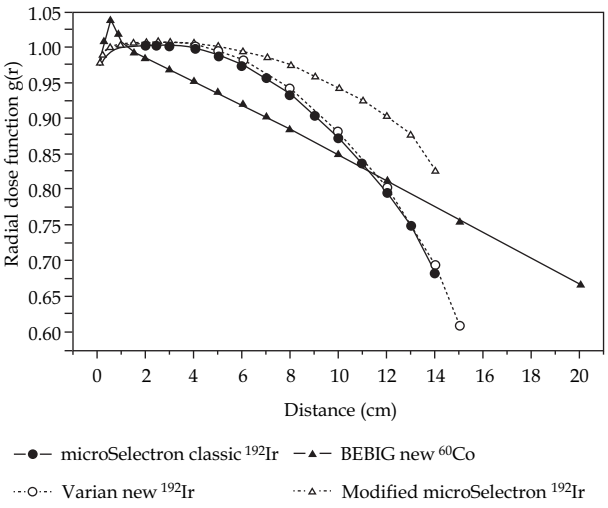


**Fig. 7.** Radial dose functions of the different HDR sources. The radial dose function of the MicroSelectron classic $^{192}$Ir source was modified to simulate a similar phantom condition as the $^{60}$Co source [17]

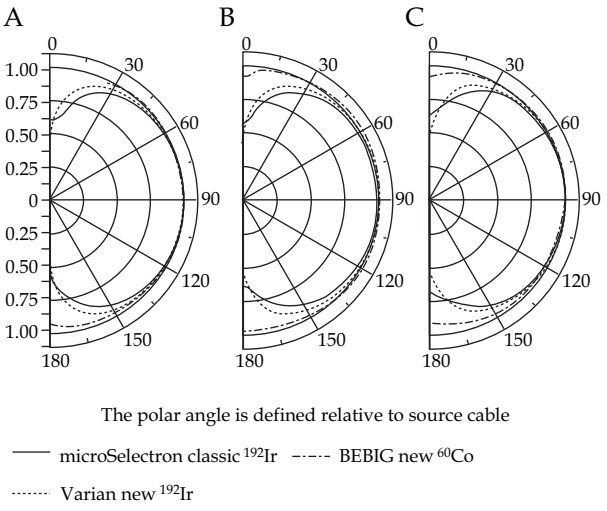


**Fig. 8.** Anisotropy functions for the different HDR sources at the distance of (A) 0.5 cm, (B) 1 cm and (C) 5 cm [17]

370 GBq. The measurement set-up consisted of a water tank with dimensions of 100 × 50 × 35 cm$^3$ in which a source holder and an ionization chamber could be moved independently. The distance to the ionization chamber could be varied up to 60 cm. The influence of smaller phantom size was studied by lowering the water level and placing foam blocks inside the tank. This allowed the width of the phantom to be altered from 18 to 50 cm. Absolute dose was measured with two ionization chambers while measurement time varied from 60 s for short distances to 600 s at larger distances. Measurements were repeated to determine the reproducibility of the set-up. The detector was placed at the perpendicular bisector of the sources to avoid anisotropy effects. In all cases the sources were considered to reflect point source configuration. All measurements were done both in air and water to calculate $T(r)$. For the Monte Carlo simulation the user code DOSRZ was used, which assumes a cylindrical geometry. It was used to calculate the energy deposited in cylindrical detectors, composed of water and situated at the axis of a large cylindrical phantom, the point sources being located at the same axis. A 20 cm radius was defined for the phantom, a 10 cm thick slab behind the source ensured backscattered radiation, while a 10 cm thick water slab at the opposite side of the simulated phantom ensured full scatter conditions [19].

Dose as a function of distance, $D(r)$ was converted into $T(r)$ using the inverse square law and normalization to unity at the distance of 1 cm. In Fig. 9 the Monte Carlo results are shown for both the $^{192}$Ir and $^{60}$Co isotope, in the range of 10-60 cm. In Fig. 10 the results of the measurements and the calculations for an infinite sized phantom are presented together for all three investigated isotopes. The influ-

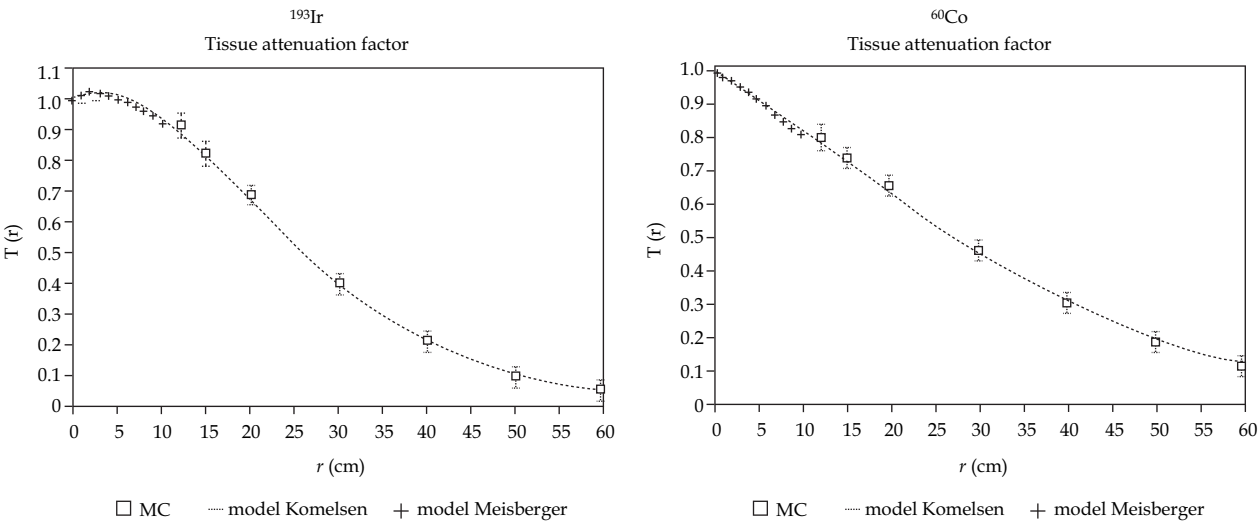


**Fig. 9.** Results of the Monte Carlo calculations for the $^{192}$Ir and $^{60}$Co isotope in the range of 10 < r ≤ 60 cm. In the range of 0 ≤ r ≤ 10 cm, results are presented from the model of Meisberger. The lines represent a fit through the Meisberger and the Monte Carlo data points, according to the model of Kornelsen [19]

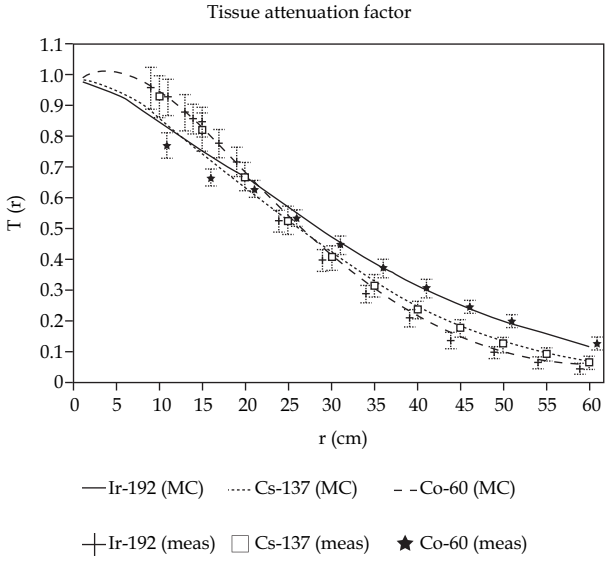


**Fig. 10.** Results of the measurements and the calculations for an infinite sized phantom, for $^{192}$Ir, $^{137}$Cs and $^{60}$Co. Results in the range of 10-60 cm obtained by measurement are presented as points. Lines are used for the Monte Carlo results [19]

ence of the dimensions of the water phantom was determined by lowering the water level and reducing the width with foam blocks. An extreme reduction of the width from 50 to 18 cm reduced the local dose by –5.4% at 15 cm source-to-detector distance and by –13.3% at 55 cm source-to-detector distance, in the case of the $^{60}$Co measurements. In the case of the $^{192}$Ir measurements, a maximum reduction in the local dose of –14% was found, when the source was brought from the centre of the phantom to 5 cm below the water surface. In all cases in which the dimensions of the phantom or the position of the source and detector were varied, reductions of this magnitude were found, compared with the measurements in the infinite phantom. From this it can be concluded that the results from the measurements in the large water phantom may be used to describe $T(r)$ for a wide range of situations. The accuracy of the measurements is determined by the accuracy with which the distance in the water phantom could be measured. Venselaar *et al.* conclude the same for both isotopes under consideration in the range of 10-60 cm from the source. A typical value of $T(r)$ for a distance of $r$ = 25 cm for all sources is approximately 0.5 and for $r$ = 50 cm, $T(r)$ is in the order of 0.15. $T(r)$ curves prove to be smooth functions for both isotopes.

### *Dose rate distributions around modern $^{60}$Co and $^{192}$Ir HDR sources*

As recommended in the updated TG-43 report by AAPM, dose distribution data of brachytherapy sources should be obtained experimentally or by the Monte Carlo algorithm. These data can then be used as input in HDR treatment planning systems. Granero *et al*. used the Monte Carlo method to obtain the dose rate distribution of a modern $^{60}$Co and $^{192}$Ir afterloading source [20].

### *Dose rate distribution around $^{60}$Co source*

Granero *et al*. investigated the dose rate distribution of a $^{60}$Co HDR source by the Bebig company (model Co0.A86) using the Monte Carlo code GEANT4 [20]. The new Bebig $^{60}$Co is very similar to the old Bebig source (model GK60M21), but the new source has a smaller active core (0.5 mm in diameter vs. 0.6 mm) and a more rounded capsule tip. It is composed of a central cylindrical active core made of metallic $^{60}$Co, 3.5 mm in length and with a diameter of 0.5 mm. The active core is surrounded by a cylindrical 0.15 mm thick stainless-steel capsule with an external diameter of 1 mm.

The source was located in the centre of a spherical water phantom of 50 cm in radius, which acts as a phantom for the $^{60}$Co source up to a distance of 20 cm from the source. The density used for the liquid water was 0.998 g/cm$^3$ at 22°C as recommended in the TG-43 report of the AAPM. To obtain the along and away dose rate table, a grid system composed of 400 × 800 cylindrical rings 0.05 cm thick and 0.05 cm high, concentric to the longitudinal source axis, was used. A system of 400 × 180 concentric spherical sections 0.05 cm thick with an angular width of 1° in the polar angle θ was used to obtain the dose rate distribution in the form given by the TG43 report. The $^{60}$Co source was located in the centre of a 4 × 4 × 4 m$^3$ air cube to estimate air-kerma strength. Kerma was scored using cylindrical ring cells, 1 cm thick and 1 cm high, located along the transverse source axis.

To obtain the TG-43 dosimetric parameters from $D(r,\theta)$ the geometric factor $G_L(r,\theta)$ with a length of $L$ = 3.5 mm has been used. The dose rate constant obtained was $\Lambda$ = 1.087 ± 0.011 cGyh$^{-1}$U$^{-1}$, where the air kerma strength is expressed in units of 1 U = 1 μGyh$^{-1}$m$^2$. The radial dose function, $G_L(r,\theta)$ is shown in Table 1 [20]. The dose rate distribution obtained for the new Bebig source has been compared with that obtained for the old Bebig HDR source; the results are depicted in Fig. 11. This comparison shows that both dose rate distributions are almost identical in front of the source; the difference between the sources is less than 0.5%.

### *Dose rate distribution around $^{192}$Ir source*

In a different study Granero *et al*. investigated the dose rate distribution in liquid water media for a $^{192}$Ir HDR source (type Ir2.A85-2). The source consists of a cylindrical pure iridium core, 3.5 mm in active length with a diameter of 0.6 mm. The source is surrounded by a capsule made of stainless steel 316 L and is very similar to other existing HDR sources. Again the Monte Carlo method was used to obtain dose rate distributions, using the GEANT4 code.

The source is immersed in the centre of a 40 cm radius water phantom, which acts as an unbounded phantom up to 20 cm of radial distance. Two different grid systems have been applied to score the kerma. The first one is used to obtain the dose rate in the form of along and away tables, $D(y,z)$; it is composed of 400 × 80 cylindrical rings with a height and width of 0.05 cm. The second grid system is used to obtain the dose distributions in polar coordinates

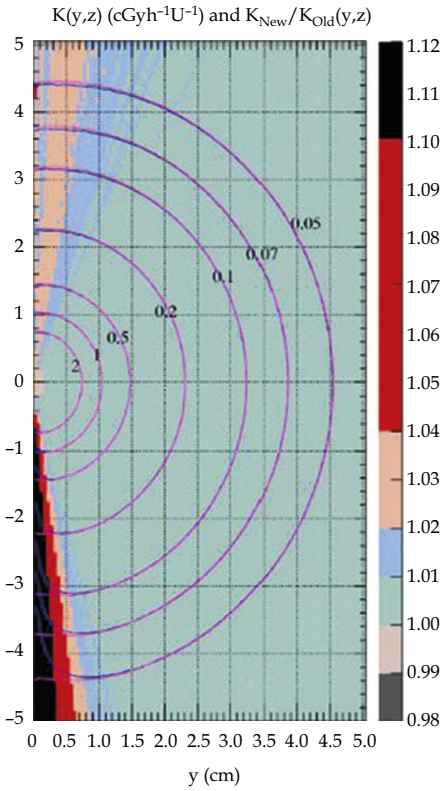


**Fig. 11.** Isodose curves in cGyh-1 U-1 for the old and the new Bebig HDR source. The background is the ratio between the kerma rate distribution [20]

$D(r,\theta)$. The air-kerma strength has been calculated to normalize the dose rate distributions in water. Therefore the HDR source was placed in a 4 × 4 × 4 m$^3$ air volume, being in composition as recommended in the updated TG-43 report of the AAPM. Air-kerma was scored along the transverse axis of the source using cylindrical cells, 1 cm thick and 1 cm high.

To obtain the TG-43 dosimetric parameters from $D(r,\theta)$ the geometric factor $G_L(r,\theta)$ with a length of $L$ = 3.5 mm was used. The dose rate constant obtained was $\Lambda$ = 1.109 ± 0.011 cGyh$^{-1}$U$^{-1}$, where the air kerma strength is expressed in units of 1 $U$ = 1 μGyh$^{-1}$m$^2$. The radial dose function $G_L(r,\theta)$ is presented in Table 2. The dose rate distribution obtained for the Bebig HDR source has been compared with that obtained for the Bebig PDR source; the results are depicted in Fig. 12.

### *Shielding*

Gamma radiation from a $^{60}$Co source is more penetrating than radiation from $^{192}$Ir and therefore different thicknesses of the same material are required to obtain identical shielding results. The higher the energy of a source, determining the penetrability, the thicker the shielding material for protection of the staff must be. The following equation is commonly used to calculate the thickness required from shielding materials to attenuate radiation to one half (the half value, HVL) or to one tenth (the tenth value layer, TVL). The half-value layers of various materials for $^{60}$Co and $^{192}$Ir are listed in Table 3 [22-24].

Instantaneous dose rates around HDR brachytherapy units with 370 GBq sources ($^{192}$Ir) made their use in conventional rooms not possible. HDR afterloading machines require special HDR facilities, which have to provide satisfactory radiation protection [25, 26].

**Table 1.** Radial dose function for the Bebig $^{60}$Co source (model Co0.A86) between 0.25 and 20 cm [20]

| Distance $r$ (cm) | GL($r$) |
|---|---|
| 0.25 | 1.007 |
| 0.5 | 1.036 |
| 0.75 | 1.015 |
| 1 | 1 |
| 1.5 | 0.992 |
| 2 | 0.984 |
| 3 | 0.968 |
| 4 | 0.952 |
| 5 | 0.936 |
| 6 | 0.919 |
| 7 | 0.902 |
| 8 | 0.884 |
| 10 | 0.849 |
| 12 | 0.813 |
| 15 | 0.756 |
| 20 | 0.665 |

**Table 2.** Radial dose function for the Bebig HDR $^{192}$Ir source (model Ir2.A85-2) between 0.25 and 20 cm [21]

| Distance $r$ (cm) | GL($r$) |
|---|---|
| 0.25 | 0.99 |
| 0.5 | 0.996 |
| 0.75 | 0.998 |
| 1 | 1 |
| 1.5 | 1.002 |
| 2 | 1.004 |
| 3 | 1.005 |
| 4 | 1.003 |
| 5 | 0.999 |
| 6 | 0.991 |
| 7 | 0.981 |
| 8 | 0.968 |
| 10 | 0.935 |
| 12 | 0.984 |
| 15 | 0.821 |
| 20 | 0.686 |

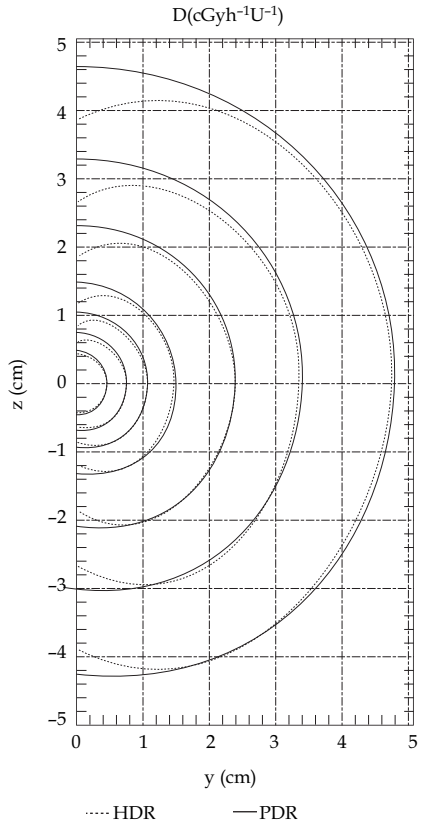


**Fig. 12.** Isodose curves in cGyh$^{-1}$ U$^{-1}$ for the HDR and the PDR source [21]

### *Experiential reports*

During the literature research for this work, talks to individual physicists of several radiation therapy institutes were conducted. Those included institutes which have already. Interviewed institutes included all radiation therapy facilities using $^{60}$Co in Germany currently and several $^{192}$Ir users in Austria. All German brachytherapy units currently equipped with $^{60}$Co used $^{192}$Ir in the past. Of those, every discussion partner mentioned that financial motives were the initial reason for a change of the radionuclide as fewer source exchanges are required using $^{60}$Co. Though no clinical results for miniaturized $^{60}$Co sources are available yet, everyone pointed out that the essential dose distributions of these isotopes are similar referring to available studies and the same clinical results are expected [9, 16, 24]. Also easier handling and quality assurance due to fewer source exchanges is widely appreciated. In most cases it was not necessary to extend radiation protection, because the therapy rooms already met radiation protection directives. One institute needed to make a development by adding an additional lead, but still calculated a return on investment after 10 years. In addition, not a single conversation partner said they would change back to $^{192}$Ir if funding would allow it now, but also mentioned that if there were no financial influence on the decision making process it would not have been considered to change the familiar system.

The situation in Austria is different, as not in a single facility is a $^{60}$Co source in operation. Many institutes are used to working with well-established $^{192}$Ir afterloading brachytherapy units. Though aware of the logistical advantages, the majority do not consider changing the existing systems. In two cases it had been contemplated to swap to $^{60}$Co sources but it was not carried out, because rebuilding would have been required to provide adequate radiation protection. One institute is planning to build new radiation therapy rooms and pointed out that the possibility to use $^{60}$Co in the future due to financial and logistical advantages will be highly considered. During all these conversations it also became obvious that the isotope is not the main basis of decision making. The equipment of the afterloader also influences the reason to purchase from a vendor, as physicians may prefer specific applicators which are not in the portfolio of the afterloader from a different company or might have gained years of experience on products of certain manufacturers. The administrative effort to deal with an increased exchange in sources is also often very well automated due to great experience and is not regarded as a burden. Thanks to many thoughts on this topic from physicists of several institutes, it cannot be assumed that the motivation to change existing systems just out of potential financial benefits is always present; much more decisive might be the satisfaction with accustomed systems.

**Table 3.** Half-value layers and tenth-value layers for $^{192}$Ir and $^{60}$Co isotopes [24]

| | Shielding thickness | | | |
|---|---|---|---|---|
| | $^{192}$Ir | | $^{60}$Co | |
| Shielding material | HVL | TVL | HVL | TVL |
| Lead | 4.83 | 16.26 | 12.45 | 41.15 |
| Steel | 15.5 | 50.8 | 22.081 | 73.66 |
| Concrete | 48.26 | 157.48 | 66.04 | 218.44 |
| Aluminium | 48.26 | 157.48 | 66.04 | 218.44 |

**Table 4.** Source used in interviewed brachytherapy departments

| Brachytherapy department | Source |
|---|---|
| Clinical centre Bayreuth, Germany | $^{60}$Co |
| Clinical centre Deggendorf, Germany | $^{60}$Co |
| Clinical centre Neumarkt, Germany | $^{60}$Co |
| Clinical centre Nürnberg Nord, Germany | $^{60}$Co |
| County hospital Gummersbach, Germany | $^{192}$Ir |
| University hospital Würzburg, Germany | $^{60}$Co |
| Clinical centre Krems, Austria | $^{192}$Ir |
| County hospital Klagenfurt, Austria | $^{192}$Ir |
| Hospital Hietzing Rosenhügel Vienna, Austria | $^{192}$Ir |
| University hospital Graz, Austria | $^{192}$Ir |
| Hospital Kaiser-Franz-Josef Vienna, Austria | $^{192}$Ir |
| Hospital SMZ-Ost Vienna, Austria | $^{192}$Ir |
| University hospital general hospital Vienna, Austria | $^{192}$Ir |

## Conclusions

Both $^{60}$Co and $^{192}$Ir isotopes have a long history in the field of brachytherapy. Several hundred HDR afterloading units equipped with $^{60}$Co or $^{192}$Ir sources have been put into use in the past. At the beginning of HDR brachytherapy $^{60}$Co was used in the form of pellets. $^{192}$Ir achieved wide acceptance as the first remote afterloading systems were introduced. The possibility of manufacturing miniaturized sources allowed HDR brachytherapy to be applied to interstitial techniques and led to a high market preference for $^{192}$Ir. The majority of temporary interstitial and intracavitary treatments in the western world now appear to be delivered by $^{192}$Ir. Still, $^{60}$Co has been widely deployed in Asia and especially in Japan for the past decades. Since $^{60}$Co is also available in miniaturized form with geometrical dimensions identical to those of $^{192}$Ir sources, it seems that there is potential to change market share. However, the higher emitting energy of $^{60}$Co photons requires increased radiation protection. The main advantage of considering $^{60}$Co for HDR brachytherapy applications is connected with the long half-life ($t_{1/2}$ = 5.27 years vs. 74 days) with source exchanges in only intervals of a few years. Despite the fact that $^{60}$Co and $^{192}$Ir sources of identical shape and dimensions have different physical characteristics, they show identical dose distributions, as demonstrated in various studies. Several dosimetric and theoretical studies support clinical equivalence of modern HDR. Differences in dose absorption in different tissues are insignificant as well. It can be assumed that there are no advantages or disadvantages of $^{192}$Ir compared to $^{60}$Co. However, simulations show that due to the higher photon energy of $^{60}$Co beyond a distance of 20 cm from the source, the integral dose is higher compared to $^{192}$Ir. The higher energy requires more room shielding for the application of a $^{60}$Co source. Many existing therapy rooms would need reconstruction regarding radiation protection. Besides, only a single company offers miniaturized $^{60}$Co HDR sources currently requiring their afterloader. The issues of reconstruction and the change of existing afterloading units will therefore not establish $^{60}$Co in the future as no clinical advantages exist. Nevertheless, there is big potential for $^{60}$Co as an alternative to $^{192}$Ir for newly constructed departments where the selection of the equipment is still in progress. The prospect of reduced costs due to fewer source exchanges will be of great interest if financial circumstances have to be considered. There may be great potential in developing countries where lots of radiation therapy facilities are still being planned. Especially the lack of experienced people for source exchange, disposal and quality assurance plays an important role. 25 source exchanges are required for $^{192}$Ir for one exchange of a $^{60}$Co source. In countries where foreign personnel must conduct these responsibilities it is even more costly. These obvious logistical advantages and potential savings will encourage other companies to make miniaturized $^{60}$Co sources available in the near future.

## Acknowledgments

Special thanks to Dipl. Ing. Peter Tonhäuser for his help, factual material and for substantive care.

## References

1. Williamson J. Brachytherapy technology and physics practice since 1950: a half-century of progress. *Phys Med Biol* 2006; 51: 303-325.
2. Levitt SH. Technical Basis of Radiation Therapy. In: Practical Clinical Applications. 4th ed. *Springer Verlag*, Berlin 2006.
3. ICRU report 38. Dose and volume specification for reporting intracavitary therapy in gynaecology. International Commission on Radiation Units and Measurements (1985).
4. Van Dyk J. The Modern Technology of Radiation Oncology. *Medical Physics Publishing*, Madison 1999.
5. Perez-Calatayud J. Monte Carlo Application in Brachytherapy Dosimetry Radiotherapy and Brachytherapy NATO Science for Peace and Security Series B: Physics and Biophysics. *Springer* 2009, Netherlands, p. 239.
6. Ning JY. Principles and practice of brachytherapy dosimetry Department of Therapeutic Radiology. *Radiat Measur* 2006; 41: 22-27.
7. Zwierzchowski G, Malicki J, Skowronek J. Dosimetric verification of dose optimisation algorithm during endovascular brachytherapy of the peripheral vessels. *Rep Pract Oncol Radiother* 2009; 14: 114-121.
8. Zwierzchowski G, Błasiak B, Stefaniak P et al. HDR and PDR 192Ir source activity control procedures, as the part of the quality assurance system at Brachytherapy Department of Greater Poland Cancer Centre. *J Contemp Brachyther* 2009; 3: 157-162.
9. Papagiannis P. Monte Carlo dosimetry of 60Co HDR brachytherapy sources. *Med Phys* 2003; 30: 712-721.
10. Baltas D. The Physics of Modern Brachytherapy for Oncology. 1st ed. *Taylor & Francis*, New York 2006.
11. Pujades-Claumarchirant MC, Granero D, Perez-Calatayud J et al. Evaluation of interpolation methods for TG-43 dosimetric parameters based on comparison with Monte Carlo data for high-energy brachytherapy sources. *J Contemp Brachyther* 2010; 2: 28-32.
12. Perez C. Principles and Practice of Radiation Oncology. 5th ed. *Lippincott Williams & Wilkins Publishing*, Philadelphia 2007.
13. Baltas D, Lymperopoulou G, Zamboglou N. On the use of HDR 60Co source with the MammoSite® radiation therapy system. *Med Phys* 2008; 35: 5263-5268.
14. Walksman R. Vascular Brachytherapy. 3rd ed. *Wiley-Blackwell*, Armonk 2002.
15. Rivard A, Coursey BM, DeWerd LA et al. Update of AAPM Task Group No. 43 Report: a revised AAPM protocol for brachytherapy dose calculations. *Med Phys* 2004; 31: 633-674.
16. Richter J, Baier K, Flentje M. Comparison of 60Cobalt and 192Iridium sources in high dose rate afterload brachytherapy. *Strahlenther Onkol* 2008; 184: 187-192.
17. Park DW, Kim YS, Park SH et al. A comparison of dose distributions of HDR intracavitary brachytherapy using different sources and treatment planning systems. *Appl Radiat Isot* 2009; 67: 1426-1431.
18. AAPM Dosimetry of interstitial brachytherapy sources AAPM Report No. 51. Report of AAPM radiation therapy committee task group 43. *Med Phys* 1996; 23: 537-543.
19. Venselaar JL, van der Giessen PH, Dries WJ. Measurement and calculation of the dose at large distances from brachytherapy sources: Cs-137, Ir-192 and Co-60. *Med Phys* 1996; 23: 537-543.
20. Granero D, Pérez-Calatayud J, Ballester F. Technical note: Dosimetric study of a new Co-60 source used in brachytherapy. *Med Phys* 2007; 34: 3485-3488.
21. Granero D, Pérez-Calatayud J, Ballester F. Monte Carlo study of the dose rate distributions for the Ir2.A85-2 and Ir2.A85-1 Ir-192 afterloading sources. *Med Phys* 2008; 35: 1280-1287.

22. Halls N. Achieving Sterility in Medical and Pharmaceutical Products. *Marcel Dekker Inc*., New York 1994.
23. Bomford CK. Therapy and Oncology. In: Walter & Miller's Textbook of Radiotherapy: Radiation Physics. *Elsevier Ltd*, London 2002.
24. Quartz L. Nondestructive Testing. ASM International, Ohio 1997; 55.
25. ICRU report. Vol. 50. Bethesda: International Commission on Radiation Units and Measurements; 1993. Prescribing, recording, and reporting photon beam therapy.
26. Nag S, Porter A, Nori D. Brachytherapy in the new millennium. In: High Dose Rate Brachytherapy: A Textbook. *Futura Publishing Co Inc*. 1997; 703-717.